



ISTITUTO NAZIONALE DI RICERCA METROLOGICA Repository Istituzionale

A Measurement System for the Characterization of Wireless Charging Stations for Electric Vehicles

Original

A Measurement System for the Characterization of Wireless Charging Stations for Electric Vehicles / Zucca, Mauro; Squillari, Paolo; Pogliano, Umberto. - In: IEEE TRANSACTIONS ON INSTRUMENTATION AND MEASUREMENT. - ISSN 0018-9456. - 70:(2021), pp. 1-10. [10.1109/TIM.2020.3046908]

Availability:

This version is available at: 11696/65110 since: 2021-01-15T12:14:56Z

Publisher:

IEEE

Published

DOI:10.1109/TIM.2020.3046908

Terms of use:

This article is made available under terms and conditions as specified in the corresponding bibliographic description in the repository

Publisher copyright

(Article begins on next page)

A Measurement System for the Characterization of Wireless Charging Stations for Electric Vehicles

Mauro Zucca¹, Senior Member, IEEE, Paolo Squillari², and Umberto Pogliano³

Abstract—This article describes a new traceable measurement system, designed for the characterization of inductive charging stations for electric vehicles. This article particularly focuses on static charging (stationary vehicle), while dynamic charging (charging while driving) requires a significantly different system. The measurement system is able to measure on-site performance and efficiency of the charging station and converters. The relative uncertainty is $\leq 10^{-3}$. The measurement system aims at accurately measure the power at the batteries and the power transferred from the ground to the onboard resonant circuit and makes possible a benchmarking between station measuring systems. Finally, this measurement system allows the characterization of the magnetic emissions by correlating them with the electric current in the coils. This system improves the ease and ability to characterize wireless charging stations both in field and laboratory environments. This article describes in detail the hardware, the software, the GPS synchronization, and, in summary, the system architecture.

Index Terms—Electric vehicles (EVs), inductive charging, measurement uncertainty, measurement.

I. INTRODUCTION

THE number of electric vehicles (EVs) has grown significantly, especially over the past years. This growth is expected to last in the next years, sustained by support policies and technological advances, although a temporary slowdown may be foreshadowed in 2020 [1]. The growth of EVs and, in particular, battery EVs (BEVs) and plug-in EVs (PEVs) places EV charging among the central issues. The situation of charging EVs is different in different countries. As an example, in Europe, not all countries have identification and communication systems for charging stations based on compatible protocols, and international interoperability is not guaranteed [2]. Another important issue is power and energy measurement traceability, which is directly related to billing. To date, there are widely different national regulations for EV metering, and this also happens in Europe. Even in this case, harmonization is needed. Moreover, charging conditions of the EV are very specific and need to be investigated and considered in specific regulations. To do so, means and

methods have to be carefully defined taking into account that there are different types of charging stations. Moreover, vehicles show different load profiles [3], and charging stations show daily, weekly, and seasonal cycles [4]. The most recent charging station typology, which is considered a pilot type, is the inductive charging technology. This technology, commonly called inductive power transfer (IPT), or wireless power transfer (WPT), has a number of obvious advantages: it is perfect for autonomous vehicles and excellent to implement in large urban centers, i.e., at the traffic lights, at work, in parking facilities, and so forth. It also makes recharging easy for people with moving disabilities and does not require the use of cables [5]–[8]. WPT charging is realized using two coils, one on the ground and one onboard, which are coupled as resonant circuits having the same frequency. The latter is unified at 85 kHz for light vehicles [9], [10] and decreases for heavy vehicles. A more futuristic version of WPT charging is the dynamic one (DWPT), which provides for charging with a moving vehicle, for example, in a road lane [11], [12]. However, DWPT needs the measurement of power and efficiency in sequences of rapidly changing regimes, which is outside the scope of our investigations.

In the framework of WPT, the accurate measurement of the power and energy transferred to the vehicle is an issue. The first proposal for a transfer power measurement is introduced in [13], where noncontact sensing elements are utilized to measure the magnetic field from WPT and calculate the power transmitted from the ground to the vehicle.

This article deals with a measuring system developed for measuring the power transferred onboard, the power transferred to the batteries, the losses at the power converters, and the overall efficiency of the system. The system is called in the following the Power Measurement Unit (PwMU), and it was developed within the project “Metrology for Inductive Charging of Vehicles” (MICEV) [14]. The system allows synchronized measurements onboard and on the ground and allows the simultaneous detection of magnetic induction levels in and around the vehicle. The system is also designed to record the waveforms of currents and voltages and the waveforms of magnetic flux density. As for the electrical measurements, which are the center of the analysis presented here, the system is able to perform electrical and efficiency measurements with an uncertainty level of no more than $\pm 1\%$ in a temperature (T) range of $18\text{ }^{\circ}\text{C} \leq T \leq 28\text{ }^{\circ}\text{C}$. Such a level of uncertainty should be sufficient to verify existing on-site measurement systems that, according to common regulations (e.g., ANSI C12.20), should be in class 0.2 or 0.5. For what concerns magnetic measurements, detailed analysis and measurement examples are reported in [15].

Manuscript received August 22, 2020; revised October 16, 2020; accepted December 7, 2020. Date of publication December 23, 2020; date of current version January 14, 2021. The results presented in this work are obtained in the 16ENG08 MICEV project, supported by the EMPIR Programme cofinanced by the Participating States and by the European Union’s Horizon 2020 Research and Innovation Programme. The Associate Editor coordinating the review process was Branislav Djokic. (Corresponding author: Mauro Zucca.)

Mauro Zucca and Umberto Pogliano are with the Istituto Nazionale di Ricerca Metrologica (INRiM), 10135 Turin, Italy (e-mail: m.zucca@inrim.it; u.pogliano@inrim.it).

Paolo Squillari is with Custom 2.0 s.r.l., 10135 Turin, Italy (e-mail: paolo.squillari@gmail.com).

Digital Object Identifier 10.1109/TIM.2020.3046908

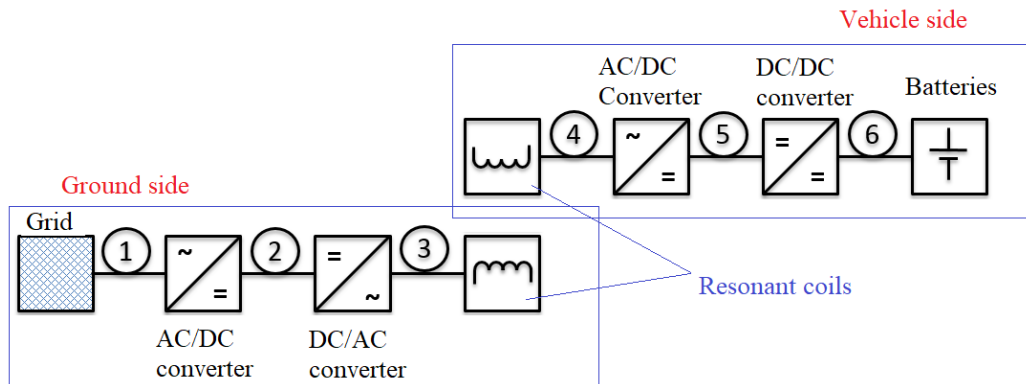


Fig. 1. Principle scheme of an IPT charging station with the vehicle. Main measurement points.

This article is an extension of [16] and is organized as follows. In Section II, the scheme of an IPT station and measurement points is shown. In Section III, the structure of the PwMU is given. In Section IV, the software user interface is presented. In Section V, the output and results' storage are described. In Section VI, the GPS synchronization is discussed. In Section VII, traceability is analyzed. In Section VIII, conclusions are reported.

II. TYPICAL IPT CHARGING STATIONS AND MEASUREMENT POINTS

The typical scheme of an IPT charging station is presented in Fig. 1. Making reference to this figure, the following holds.

- 1) The charging station on the ground consists of a connection point to the electricity grid, usually a three-phase connection in point (1). An ac/dc converter follows, the output of which connects to a dc/ac converter in point (2), which supplies the transmission coil (TX coil) in point (3) at a resonant frequency of 85 kHz in the case of light vehicles (various types of cars) or between 20 and 30 kHz in the case of heavy vehicles (trucks or buses).
- 2) The charging station on the vehicle consists of the receiving coil (RX coil) working at the same resonant frequency of the coupled TX coil. The RX coil output, that is point (4), is connected to an ac/dc converter providing the dc power for batteries in point (5). Sometimes, there is another dc/dc converter that connects the batteries at point (6).

The measurement system was designed to perform the following functions: 1) to measure the power absorbed from the charging station by the load in point (5) or (6), i.e., batteries; 2) to measure the power absorbed by the charging station from the electric grid in point (1); 3) to determine the synchronized ratio between the two power quantities mentioned above (overall efficiency); 4) to measure the power transferred to the vehicle in point (3); 5) to measure the power received by the vehicle in point (4); 6) to measure the efficiency of power converters, e.g., the ratio of the power between point (3) and point (1) or between point (6) and point (4); 7) to measure the magnetic induction levels in the charging station;

and 8) to record all measured values and waveforms in their measurement time interval.

The PwMU performs measurements onboard, being voltages up to 1000 V and currents up to 200 A in the dc section. For the grid side (three-phase), the magnitude of the phase voltages is up to 400 V, and that of the phase currents is up to 200 A. In both cases, the target power is 200 kW.

In addition to these functions, the measurement system is able to measure the currents, voltages, and power at the resonant circuits, both on the ground and onboard side (ac signals).

Finally, a specific module has been created for the measurement of magnetic flux density inside and around the vehicle. Also, this module is able to record all measured values and induction waveforms and to synchronize the magnetic induction waveforms to that of the currents in the coils. The latter function is particularly important for the validation of magnetic field measurements and the verification of human exposure models, which asks for a certain correlation between electric current and magnetic induction.

III. STRUCTURE OF THE PwMU

The PwMU is constituted of three units plus numerous accessories and transducers.

- 1) One unit designed to stay on the ground side and perform measurement of the power, voltage, and current adsorbed from the grid, which we will call the "Grid Unit" (GU).
- 2) One unit that can be embarked onboard the vehicle that we will call it "Board Unit" (BU), which can also measure the signal with high-frequency components in the Ground Side (point 3, Fig. 1).
- 3) One unit that an operator can easily move in the charging station, around and inside vehicles, for magnetic field measurements, which we will call "Magnetic Unit" (MU).
- 4) In addition to the three logical units, the PwMU is accompanied by a system of two laptops, sensors, and transducers, which includes connectors, shunts, cables, and three GPS antennas, whose importance is not negligible.

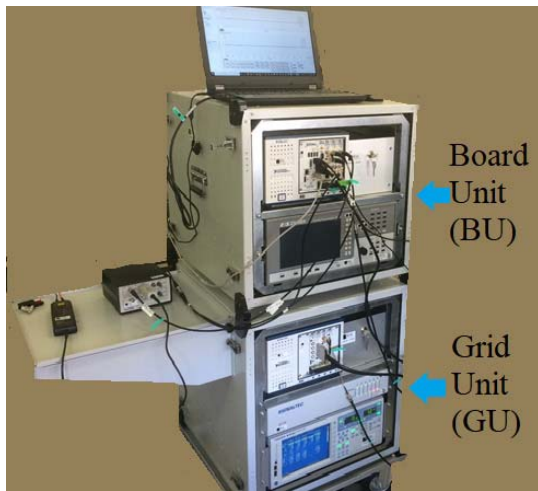


Fig. 2. Main modules of the PwMU.

In static measurements, which mainly concern this article, BU and GU can be stationed in the same place. For their housing, a double-rack has been designed for the purpose so that the two units can be stacked and moved on wheels. If necessary, they can be separated.

A specific constructive choice was made in the project. In fact, the measurement system is designed for measurements at the charging stations. The need for transporting the instrumentation and the complexity of the measurements require a reliability check in the field. Thus, also, to avoid doubts about the measurement, the presence of a second measurement system may be useful. For this reason, GU and BU are each equipped with two different measurement systems, which are described in Sections III-A and III-B, respectively.

A. Grid Unit

As stated earlier, the GU, as well as the BU, was conceived with two measurement systems, so as to have redundancy and better reliability during in-field measurements. Instruments are housed in a specific modular rack (lower cabinet) with shock absorbers and waterproof lids for transport, with braked wheels and an additional shelf (see Fig. 2).

In the GU, the first measurement system consists of a four-channel Yokogawa WT 3000 power analyzer, which is used with LEM current transducers and direct voltage input.

The second measurement system consists of a National Instruments PXI device slot chassis, based on NI PXIe-6366 and NI PXI-6683H acquisition cards, connected to current and voltage transducers. The NI PXIe-6366 Multifunction DAQ 8 simultaneous analog inputs at 2 MS/s/ch with the 16-bit resolution are utilized to acquire the three-phase voltages and the three-phase currents from the transducers described in the following, by means of a shielded I/O block connector, SCB-68, prewired with BNC outputs. The active power is computed real time via software, calculating for each phase the instantaneous power and averaging it every 200 periods.

Calculations are performed using a laptop processor connected to the measurement system by means of an MXI express card PCIe-8361. The GPS NI PXI-6683H, IRIG-B,



Fig. 3. Main accessories of the PwMU.

IEEE 1588, and 16-MS/s card provide the timestamp for the synchronization with the BU, by means of a GPS antenna with a 30-meter cable. The transducer system is based on a Signaltec Signal conditioner MCTS2/6 Channel using both LEM ultrastab IT 65-s ac/dc current transducers or LEM ultrastab IT 205-s ac/dc current transducers, depending on the rated power of the charging station. To measure voltages, the PXI system uses Tektronix P5200A active voltage differential probes. The main probes, transducers and GPS antennas are shown in Fig. 3.

B. Board Unit

Also, the BU has been conceived with two measurement systems. They are housed in a specific modular rack (upper cabinet in Fig. 2) with shock absorbers and waterproof lids for transport. The cabinet can be moved to the vehicle if necessary.

The first measurement system consists of a Zimmer LMG 670 power analyzer, which is used with Guildlines 7340 Series, and ac/dc current calibration standards coaxial shunt and direct voltage input. The system is conceived for single-phase measurements, even if additional two channels are available at the power analyzer.

The second measurement system consists of a National Instruments PXI device based on a NI PXIe-1071 chassis with NI PXI 8840 Controller with Windows 10 and Labview onboard. Two synchronized NI PXIe-5922 oscilloscope cards provide four input channels for voltages and currents from transducers. These cards were chosen among other reasons because they have a very limited skew between channels, <500 ps, once synchronized. The latter are LEM Ultrastab IT 65-s or IT-205-s ac/dc current transducers and Tektronix active voltage differential probes P5205A plus Tektronix 1103 amplifier for P5205A probes.

Also, in this case, the GPS NI PXI-6683H provides the timestamp for the synchronization with the BU, by means of a GPS antenna with a 30-m cable.

C. Magnetic Unit

The MU is designed to perform magnetic induction measurements in a charging station. As a complementary facility, a positioning system can be useful to place the magnetic

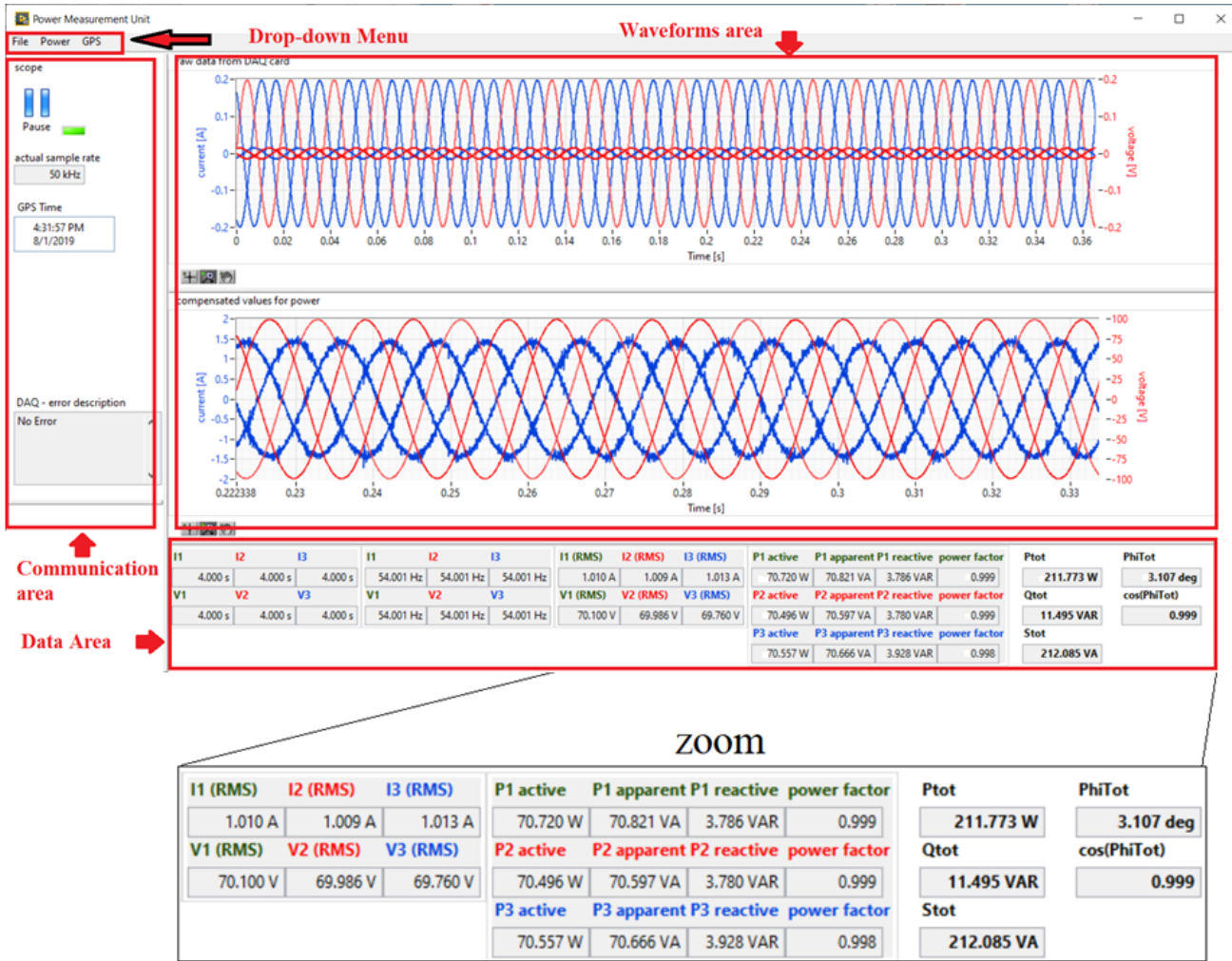


Fig. 4. GU main user interface display.

field sensor correctly, in charging stations significant points, onboard and around a vehicle.

The MU consists of the following components:

- 1) a magnetic induction meter NARDA ELT-400 with two probes: one of 100 cm² and another of 3 cm²;
- 2) an acquisition system, based on a PXI chassis that houses, among other things, two NI PXI 5922 oscilloscope cards that provide three channels for acquiring the magnetic induction components from the ELT-400 through a signal cable with BNC output;
- 3) an NI PXI-6683 GPS card, to manage the synchronization functions, useful for example to associate the measurement of the magnetic field to that of the currents in the resonant coils that are the main source of magnetic emissions;
- 4) a GPS antenna with cable;
- 5) a laptop for the management, through a LabVIEW program developed for the purpose, of the synchronization, acquisition, and data saving program.

The length of the GPS cable (30 m) and that of the signal cable (5 m) allow one to move the magnetic field meter with a certain freedom in a wide space, reducing the movements of the PXI system and the laptop to a minimum.

The scheme and more details on the MU are reported in [15], together with the measurement uncertainty assessment and an example of application in two charging stations. In this article, we will mainly focus on the other two units, BU and GU.

IV. SOFTWARE USER INTERFACES

The GU and the BU user interfaces have been developed in the LabVIEW language.

A. GU User Interface

The user space of the GU user interface (see Fig. 4) is constituted by a drop-down menu, one communication area, a waveforms area, and a data area. The drop-down menu includes the following choices.

1) *File*: It allows the user to save a nonsynchronized measurement or exit the program.

2) *Scope*: It allows the user to set the time span of the acquisition, the sample rate, the channel coupling, the input impedance of the channels, and some minor parameters, such as the vertical range.

3) *Power*: It allows the user to set the gains of the six current and voltage transducers of the PXI measurement system.

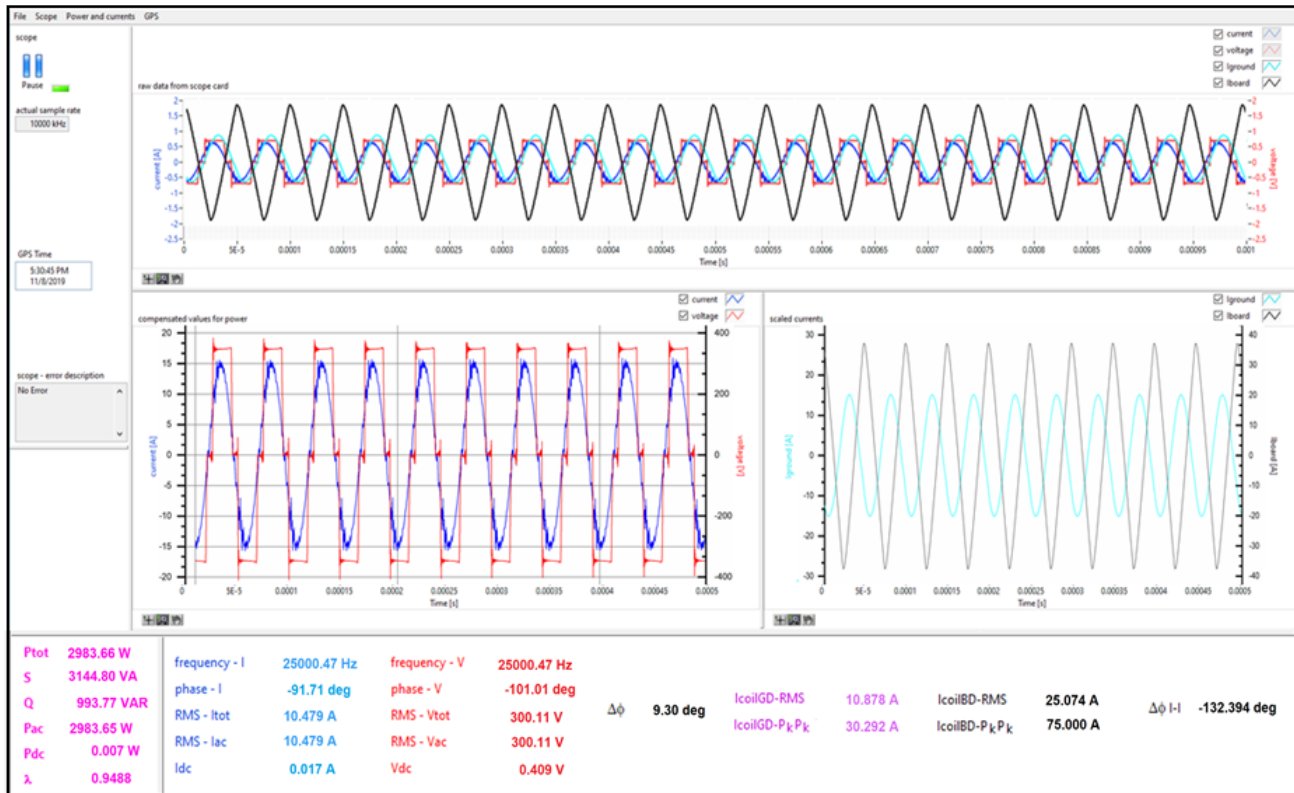


Fig. 5. BU main user interface display.

4) *GPS*: It allows the user to programmatically set the instant of measurement and related acquisition.

In the waveforms area, there are two distinct subareas. In the first, currents and voltages are shown as a raw measurement of the transducers. In the second subarea at the bottom, the actual currents and voltages are shown, calculated with the appropriate gains set in the software.

In the data area, for each current and voltage, the sampling period and the measured frequency are shown. In the same area, the rms value of each current and voltage is shown, together with the power factor and the active, reactive, and apparent powers for each phase. Finally, also, the total active power, the total reactive power, and the total apparent power are shown, together with the total phase angle and the total power factor. During the measurements, the display of the waveform and the calculated parameters is continuously updated.

In the communication area, it is possible to pause the display, see the actual sample rate, see the GPS time possibly set for a synchronized acquisition, and see any problem in the execution of the acquisition program.

The user can register an acquisition at any time via the file menu. When it is necessary to perform a synchronized acquisition, for example, to determine the efficiency of the system with a simultaneous measurement of the BU, the acquisition time instant can be set through the GPS drop-down menu.

The menu "Power" allows to set the sample rate and the acquisition time span and allows the correction of the current and voltage transducers when transducers are utilized and

a correction matrix is available. This is usually not needed when power frequency measurements are performed since the transducer accuracy is sufficient.

B. BU User Interface

As the GU, also the BU user interface has been developed in LabVIEW language. Also here (see Fig. 5), the user space is constituted of a drop-down menu, one communication area, a waveforms area, and a data area. The drop-down menu includes the following choices.

- 1) *File*: It allows the user to save a nonsynchronized measurement at any time or exit the program.
- 2) *Scope*: There are two drop-down menus.
 - a) The first one allows the user to set, among other quantities, the channel input impedance, the vertical coupling, and the vertical range and to enable/disable the channel.
 - b) The second one allows to set the sample rate and the acquisition time span.
- 3) *Power (Power and Currents)*: There are drop-down menus.
 - a) The first one allows the user to set the gains of the current and voltage transducers. This can be done by forcing a constant gain (not very useful for voltage transducers) or uploading three calibration matrixes to correct phase error and ac and dc gains. Calibration matrixes have many rows, each one corresponding to amplitude, and many columns,

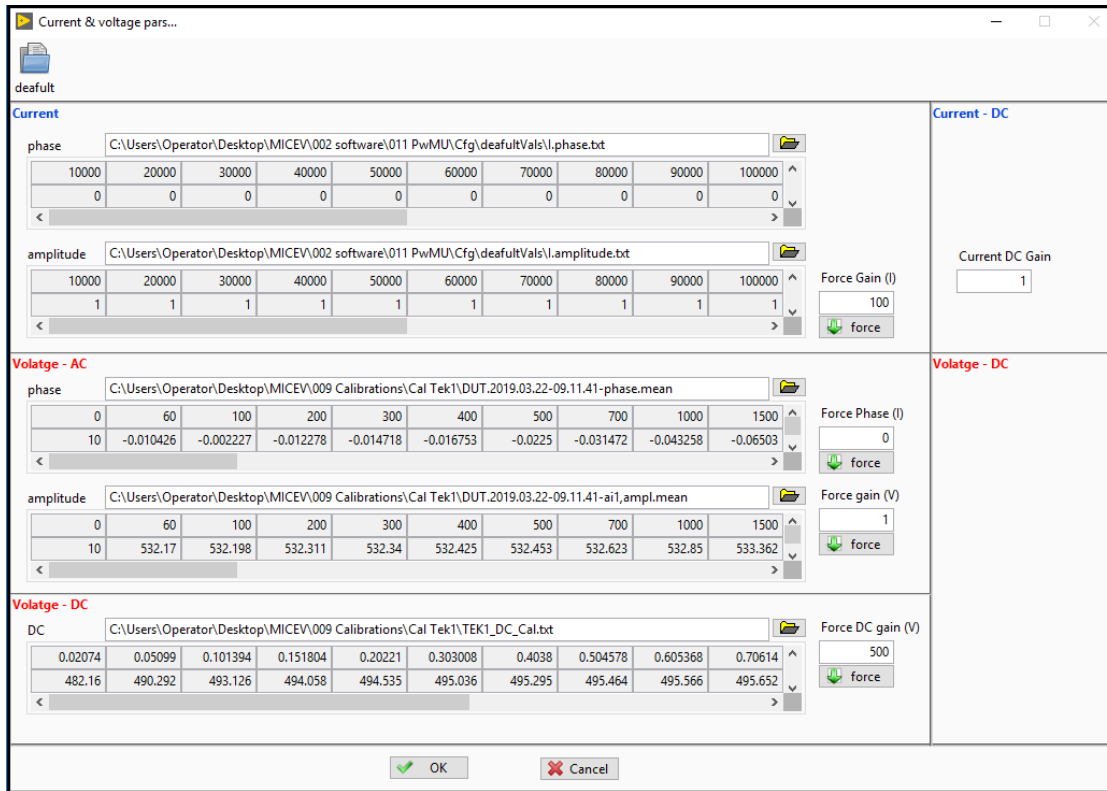


Fig. 6. Example of the interface for the calibration matrix of sensors. Upload can be done either by a.txt or.csv file, or manually.

each one corresponding to a frequency in hertz. The dc gain matrix has only two rows and many columns reporting the sensor dc output and the corresponding gain (see Fig. 6). The procedure to obtain the calibration matrix for voltage sensors is described in [17] and [18].

b) The second one allows the user to enable a popup that, through the network port, shows the power analyzer measured power, current, and voltage. If the onsite calibration has been performed correctly, discrepancies between the PXI system and power analyzer have to be limited to a few parts per thousand.

4) *GPS*: It allows the user to programmatically set the instant of measurement. The menu is the same for the GU and MU. A popup appears (see Fig. 7) where the current date (or possibly also on another date if necessary) and the instant (hours, minutes, and seconds) of the acquisition can be set. When the “OK” key is pressed, the trigger instant appears in the communication area according to the logic shown in Section VI.

As in the GU, also in the BU during the measurements, the display of the waveform and the calculated parameters is continuously updated, and in the communication area, it is possible to pause the display and to see any warning. The efficiency of the system, overall or partial, is obtained from GU and BU simultaneous measurement performed by means of the GPS drop-down menu. When the trigger instant is reached, the acquisition starts, and at the end of the sampling

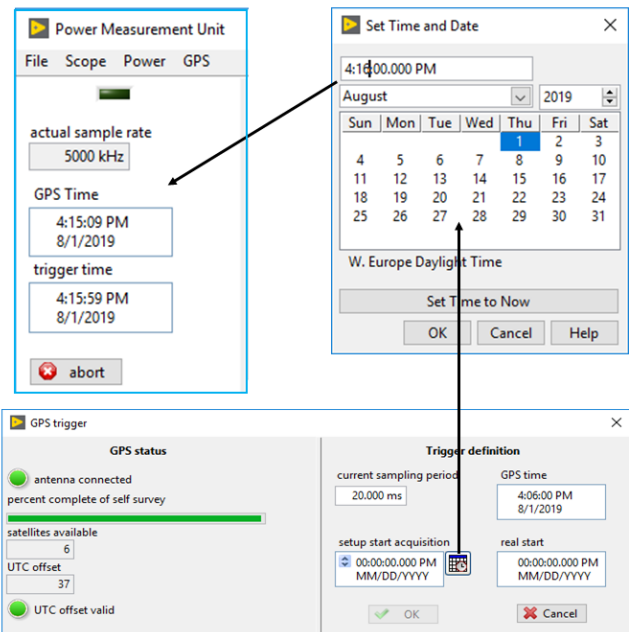


Fig. 7. The menu where the operator can set the acquisition instant (trigger time).

period, quantities are saved, according to what is described in Section V. A popup communicates that the execution of the measurement is done, and the data have been recorded. From the recorded data at the same timestamp in the GU and BU units, the efficiency can be obtained.

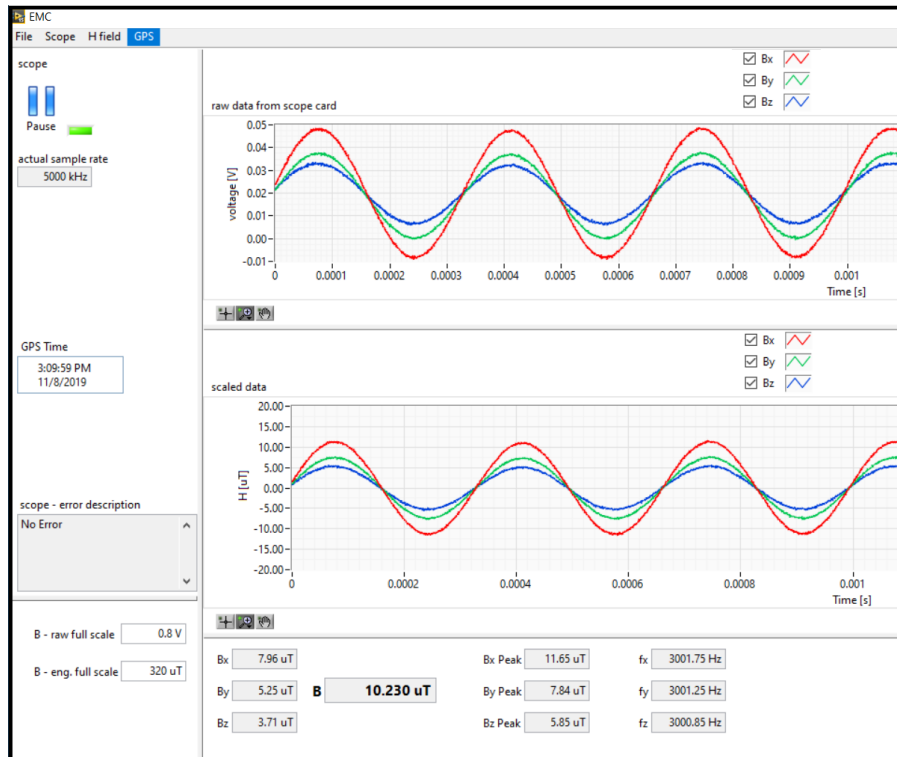


Fig. 8. MU user interface main display.

C. MU User Interface

The user space is similar to one of the other units (see Fig. 8). The parameters of the magnetic field meter, voltage range (raw full scale), and measurement range are set directly in the user interface between the communication and data areas.

The drop-down menu allows the user to save a nonsynchronized measurement or exit the program, while the “Channels” menu allows the user to set, among other quantities, the input impedance of the acquisition card, the vertical coupling, and the vertical range and to enable/disable the channel. The “Horizontal” menu allows to set the sample rate and the acquisition time span. The H-field menu allows to visualize the quantities in terms of magnetic field or magnetic induction, while the “GPS” menu is conceived as in the other units.

V. OUTPUT AND RESULTS’ STORAGE

The measurement data can be saved by the user in two ways: 1) freely, at any time or 2) with a programed measurement (synchronized), via GPS. In both cases, the file structure does not change; however, the file name changes. It will be the following.

- 1) *Unit*: yyyy.mm.dd-hh.mm.ss.tdms.
- 2) *GPS Trigger-Unit*: yyyy.mm.dd-hh.mm.ss.tdms.

Here, the unit can be GU or BU or MU, and yyyy.mm.dd is the date (year, month, day) and dd-hh.mm.ss time (hour, minute, second) coming from the GPS timestamp in both cases. In this way, each acquisition will have a unique identification and will contain a record of the date and time of measurement.

The file structure is the same in both cases. The Technical Data Management Streaming (tdms) format was chosen because it is compact and can be read by general-purpose programs, such as Microsoft Excel, through the installation of a simple plugin.

The file consists of four main tabs.

- 1) The first tab shows the GPS timestamp, the record length for each registered channel, the channel names, the associated quantities, and the sampling frequency.
- 2) The second tab shows the columns with the “raw” data acquired by the sensors, e.g., currents and voltages I_i^* U_i^* or magnetic flux densities B_i^* in the case of MU, which were not multiplied by the gains previously set in the software.
- 3) The third tab shows six columns with the real quantities (through the transducers gains).
- 4) The fourth tab shows all the quantities computed real time, which is shown in the data area. This includes the frequency, the total power (active, reactive, apparent, and power factors), and all the measured and calculated summary parameters (for each phase in the case of ground measurement), including the rms value of voltages and currents.

VI. GPS SYNCHRONIZATION

For the synchronization, two possibilities were considered: the adoption of a single GNSS-disciplined clock in order to synchronize all the units through a suitable protocol, for example, through the IEEE 1588 protocol, which is a packet-based two-way communications protocol specifically designed to

synchronize distributed clocks on an Ethernet or IP-based network. A second considered possibility was to equip each unit of the PwMU with an independent synchronization system, referable to a specific synchronization instant settable by the user through GNSS synchronization.

To make the PwMU units synchronized but independent, the second solution was adopted, which also enables the PwMU to be synchronized with any external GNSS system, without any need for software modification.

The solution adopted was that of GPS synchronization, by using a PXI-6683H card on the PXI chassis of each unit. All the GPS antennas are mounted on the same holder.

A. Adopted Solution

In order to have synchronous acquisitions, first, it is necessary to connect the oscillators of the interested PXIs through a wireless communication protocol. The GPS (through the PXI-6683H card) is accurate and allows to reach a time synchronization uncertainty of 50 ns. In detail, the PXI-6683H hooks up to GPS satellites and provides a pulse per second (PPS) signal, which is used to lock a 10-MHz clock in phase, which, in turn, can be used as a time base for the various acquisition boards. The routing of this clock on the PXI backplane can be easily done.

The GPS synchronizes the clocks of the different PXI. The PXI-6683H cards can be programmed to provide a trigger start signal on the PXI backplane at a certain time (ES: 11:00:00 AM). All the systems are started together, but they obviously inherit the GPS uncertainty, ± 50 ns.

For the PwMU, the sampling time can be of the order of tens of microseconds (onboard) up a few seconds (ground side). This allows one to neglect the drift between clocks since the measurement is quick and clock drifting negligible.

In the case of long acquisitions (minutes, hours, or days), further synchronization steps are required to avoid drifting, and the compensation for the PLL board coupling delay is required, which, in this case, is not necessary. In conclusion, between two different chassis, the synchronization uncertainty is ≤ 100 ns. This value, given the sampling times described in the following paragraph, does not involve problems for the calculation of the charging efficiency.

B. Synchronization Between Units

Synchronization occurs by setting, on each unit to be synchronized, the same instant of acquisition t_0 (e.g., 11.00.00 A.M.). The operator of a unit must communicate to that of the other units the moment of acquisition chosen, and this normally takes place about 1 min before the acquisition.

On each unit u , a sampling period during $\Delta T_{(u)}$ is set. The initial acquisition instant will be

$$t_i = t_0 - \frac{\Delta T_{(u)}}{2} \quad (1)$$

while the final is computed according to formula (2)

$$t_f = t_0 + \frac{\Delta T_{(u)}}{2}. \quad (2)$$

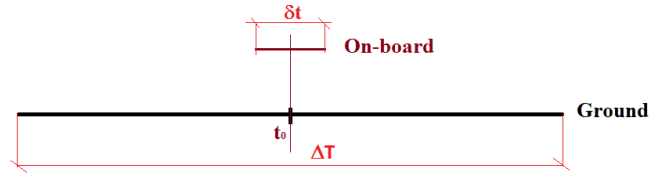


Fig. 9. Example of synchronization of two measurement units, at the instant t_0 , depending on their sampling period.

The duration of the sampling period can be different. For instance, for the ground unit that needs to sample a signal at power frequency, the default sampling period is 4 s: $\Delta T_{(GU)} = \Delta T = 4$ s.

The sampling period of 4 s is set equal for both the GU measurement devices: the Yokogawa WT3000 and the GU PXI system.

As for the BU, where the frequency can be 25 or 85 kHz typically, the sampling period is typically $\Delta T_{(BU)} = \delta t = 20$ ms.

The sampling period of 20 ms is set equal for both the BU measurement devices: the Zimmer LMG-670 power analyzer and the BU PXI system.

The two sampling periods are very different but are centered, according to what is represented graphically by Fig. 9.

Conventionally, the name of the saved file (see Section V) always shows the initial instant of formula (1), t_i .

VII. TRACEABILITY

A. Traceability of the BU

The BU is called to perform dc measurements in the presence of high-frequency disturbances to measure the power at the vehicle batteries or, possibly, also to assess the power in the resonant circuits. This involves measuring signals in the range of 20–100 kHz and possibly up to 150 kHz.

In order to have traceability for this type of measurement, a Zimmer LMG 670 power analyzer combined with LEM 205-S Ultrastab current transducers with Signaltec MCTS signal conditioner was chosen as the first choice. Such transducers are very common in most research laboratories in the automotive sector.

A preliminary calibration of the Zimmer system plus current transducer was done at the Research Institute of Sweden (RISE), up to 100 kHz. The results show quite high uncertainty due to the variation of the transducer gain according to the position of the cable inside the transducer hole. This issue, which is negligible at power frequency (50 or 60 Hz), increases at increasing frequency. To overcome this problem, two Guildline 7340-100 and ac/dc current calibration standards coaxial shunts were included in the system (one in use and one for backup) providing high stability and high accuracy up to 100 kHz (angle error $< 0.15^\circ$ and uncertainty < 100 ppm at 100 kHz). A further calibration performed at German NMI (PTB), with this second configuration, provided a measurement uncertainty lower than 0.1%.

The second measurement system (PXI-based) implements an LEM 65 or 205-S Ultrastab current transducers.

To overcome the problem of the slight gain variation of the transducers during onsite measurement, when the cable has been positioned inside the transducer (and its position is no longer modified), one can proceed as follows.

- 1) The measurement of voltage, current, and power is performed with both systems.
- 2) The ratio r between the rms value of the current measured with the Zimmer power analyzer through the Guildline shunt (I_z) and the current measured by the PXI system through the current transducers (I_{cur}) is computed according to formula (3)

$$r = \frac{I_z}{I_{\text{cur}}}. \quad (3)$$

- 3) The rated gain g of the current transducer is corrected via software from g to g^* according to formula (4)

$$g^* = r \cdot g. \quad (4)$$

Through this “tuning” procedure of the current meter of the second system, the two systems provide congruent measurements, with differences limited to a hundred ppm at the highest frequencies (85 kHz) and negligible difference (few ppm) in dc.

B. Traceability of the GU and MU

Traceability of the GU is guaranteed by the Yokogawa power analyzer together with current the LEM current transducers that have been calibrated together at power frequency. At room temperature, the measurement uncertainty is ≤ 50 ppm. The PXI system and Yokogawa power analyzer provide power measurements that are in agreement. Relative discrepancies tested in the laboratory are lower than 0.02%. The MU accuracy and traceability are discussed in [15].

C. Further Investigation

The assessment of the measurement uncertainty of the system during in-field measurements, the effect of harmonic distortion and conducted disturbances, and the effect of temperature are discussed in the companion article [19].

VIII. CONCLUSION

The on-site characterization of charging stations for EVs, both for the verification of their measurement systems and for the verification of their efficiency, will be a topic of growing interest in the years to come. This article has proposed a reliable and accurate measurement system for the study and verification of IPT vehicle charging stations. Compared with the stations for wired charging, wireless charging requires a more complex system, especially for the presence of the high-frequency resonant coupling circuit, which also requires verification of the magnetic induction levels near the coils and inside the vehicle. In order to be reliable and accurate, the system requires the use of a lot of high-end instrumentation, including power analyzers and magnetic induction meters and synchronization systems. Of course, one of the challenges of the years to come will also be to make measurement and verification systems cheaper, which can be done on the basis of the experiences gradually gained.

ACKNOWLEDGMENT

The results presented in this article are developed in the framework of the 16ENG08 MICEV Project.

REFERENCES

- [1] *Global EV Outlook 2020 Entering the Decade of Electric Drive?* IEA, Paris, France, Jun. 2020.
- [2] R. Ferwerda, M. Bayings, M. van der Kam, and R. Bekkers, “Advancing E-roaming in Europe: Towards a single ‘language’ for the European charging infrastructure,” *World Electr. Vehicle J.*, vol. 9, no. 4, p. 50, 2018.
- [3] H. Neue, S. Deters, and R. Saiju, “Analysis of electrical charging characteristics of different electric vehicles based on the measurement of vehicle-specific load profiles,” in *Proc. NEIS Conf. Sustain. Energy Supply Energy Storage Syst.*, Hamburg, Germany, Sep. 2019, pp. 1–6.
- [4] K. N. Hasan, K. M. Muttaqi, P. Borboa, J. Scira, Z. Zhang, and M. Leishman, “Measurement-based electric vehicle load profile and its impact on power system operation,” in *Proc. 9th Int. Conf. Power Energy Syst. (ICPES)*, Dec. 2019, pp. 1–6.
- [5] D. Kishan and P. S. R. Nayak, “Wireless power transfer technologies for electric vehicle battery charging—A state of the art,” in *Proc. Int. Conf. Signal Process., Commun., Power Embedded Syst. (SCOPES)*, Oct. 2016, pp. 2069–2073.
- [6] V. Cirimele, M. Diana, F. Freschi, and M. Mitolo, “Inductive power transfer for automotive applications: State-of-the-art and future trends,” *IEEE Trans. Ind. Appl.*, vol. 54, no. 5, pp. 4069–4079, Sep. 2018.
- [7] S. Li and C. C. Mi, “Wireless power transfer for electric vehicle applications,” *IEEE J. Emerg. Sel. Topics Power Electron.*, vol. 3, no. 1, pp. 4–17, Mar. 2015.
- [8] Y.-C. Hsieh, Z.-R. Lin, M.-C. Chen, H.-C. Hsieh, Y.-C. Liu, and H.-J. Chiu, “High-efficiency wireless power transfer system for electric vehicle applications,” *IEEE Trans. Circuits Syst. II, Exp. Briefs*, vol. 64, no. 8, pp. 942–946, Aug. 2017.
- [9] J. Schneider, “Wireless power transfer for light-duty plug-in/electric vehicles and alignment methodology,” SAE Tech. Paper J2954_201605, 2016.
- [10] *WPT for LightDuty PlugIn/ EVs and Alignment Methodology*, SAE TIR Standard J2954, May 2016.
- [11] S. Laporte, G. Coquery, V. Deniau, A. De Bernardinis, and N. Hautiere, “Dynamic wireless power transfer charging infrastructure for future evs: From experimental track to real circulated roads demonstrations,” *World Electr. Vehicle J.*, vol. 10, no. 4, p. 84, 2019.
- [12] V. Cirimele, F. Freschi, L. Giaccone, L. Pichon, and M. Repetto, “Human exposure assessment in dynamic inductive power transfer for automotive applications,” *IEEE Trans. Magn.*, vol. 53, no. 6, Jun. 2017, Art. no. 5000304.
- [13] S. Y. Chu and A.-T. Avestruz, “Transfer-power measurement: A non-contact method for fair and accurate metering of wireless power transfer in electric vehicles,” in *Proc. IEEE 18th Workshop Control Modeling Power Electron. (COMPEL)*, Stanford, CA, USA, Jul. 2017, pp. 1–8.
- [14] M. Zucca *et al.*, “Metrology for inductive charging of electric vehicles (MICEV),” in *Proc. AEIT Int. Conf. Electr. Electron. Technol. Automot. (AEIT AUTOMOTIVE)*, Jul. 2019, pp. 1–4.
- [15] I. Liorni *et al.*, “Assessment of exposure to electric vehicle inductive power transfer systems: Experimental measurements and numerical dosimetry,” *Sustainability*, vol. 12, no. 11, p. 4573, Jun. 2020.
- [16] M. Zucca, P. Squillari, and U. Pogliano, “A measurement system for the characterization of wireless charging stations for electric vehicles,” in *Proc. Conf. Precis. Electromagn. Meas. (CPEM)*, Denver, CO, USA, Aug. 2020, pp. 1–2.
- [17] M. Zucca, U. Pogliano, M. Modarres, D. Giordano, G. Crotti, and D. Serazio, “A voltage calibration chain for meters used in measurements of EV inductive power charging,” in *Proc. Conf. Precis. Electromagn. Meas. (CPEM)*, Jul. 2018, pp. 1–2.
- [18] M. Zucca, M. Modarres, U. Pogliano, and D. Serazio, “1-kV wideband voltage transducer, a novel method for calibration, and a voltage measurement chain,” *IEEE Trans. Instrum. Meas.*, vol. 69, no. 4, pp. 1753–1764, Apr. 2020.
- [19] M. Zucca *et al.*, “Electrical measurements at inductive charging stations for electric vehicles. An outcome from Micev project,” in *Proc. Conf. Precis. Electromagn. Meas. (CPEM)*, Denver, CO, USA, Aug. 2020, pp. 1–2.



Mauro Zucca (Senior Member, IEEE) was born in 1968. He received the Ph.D. degree in electrical engineering from Politecnico di Torino, Turin, in 1998.

He received the qualification as an associate university professor in 2014 and the qualification as a senior researcher in 2017. He is currently a Senior Researcher with the Istituto Nazionale di Ricerca Metrologica (INRIM), Turin, Italy, where he is also the Head of the Electromagnetic Devices Laboratory. He is the author/coauthor of more than 100 articles,

the majority on ISI peer-reviewed journals. He is a coauthor of three patents, an international technical guide, and commercial software. Since 2005, he has been involved in 12 cooperative research projects. He was a principal investigator of three research projects. His main research activities are electrical metrology, with a particular interest in voltage measurements, electromagnetic modeling, magnetoelastic systems, shielding, and medical devices devoted to transcranial stimulation.

Dr. Zucca has been serving as a reviewer for several journals.



Umberto Pogliano was born in Turin, Italy, in 1950. He received the Dr.Ing. degree in electronic engineering and the Ph.D. degree from the Politecnico di Torino, Turin, in 1975 and 1987, respectively.

In 1977, he joined the Electrical Metrology Department, Istituto Nazionale di Ricerca Metrologica (INRIM), Turin, where his research activity was focused on the development of systems and procedures for precision dc and ac low-frequency measurements. His main interests were in the ac-dc transfer standard, in the ac voltage, current, and power measurements, and in the generation, acquisition and reconstruction of electrical signals. In 2015, he retired but still cooperates as a metrology expert in some INRIM projects and activities.



Paolo Squillari was born in Turin, Italy, in 1972.

He has been a Technician with the Dipartimento Energia (DENERG), Politecnico di Torino, Turin, since 1999, where he has been a freelancer since 2005. He develops software for research and development projects using LabVIEW for both the Politecnico di Torino and private companies. He is also a Certified LabVIEW Developer (CLD) and a Certified Professional Instructor (CPI) for NI, formerly National Instruments Corporation, Austin, TX, USA. He trains LabVIEW for NI. His develop-

ment areas include electrical metrology, automotive, fuel cells, and test rig automation.